Elucidation of roles for vitamin B_{12} in regulation of folate, ubiquinone, and methionine metabolism

Margaret F. Romine[a,1], Dmitry A. Rodionov[b,c,1], Yukari Maezato[a,1], Lindsey N. Anderson[a], Premchendar Nandhikonda[a], Irina A. Rodionova[c,2], Alexandre Carre[d], Xiaoqing Li[c], Chengdong Xu[a], Therese R. W. Clauss[a], Young-Mo Kim[a], Thomas O. Metz[a], and Aaron T. Wright[a,3]

[a]Biological Sciences Division, Pacific Northwest National Laboratory, Richland, WA 99352; [b]Department of Microbial Genomics, A. A. Kharkevich Institute for Information Transmission Problems, Russian Academy of Sciences, Moscow 127994, Russia; [c]Department of Bioinformatics, Sanford-Burnham-Prebys Medical Discovery Institute, La Jolla, CA 92037; and [d]Department of Bioengineering, Polytech Nice-Sophia, 06410 Biot, France

Edited by Benjamin F. Cravatt, The Scripps Research Institute, La Jolla, CA, and approved December 29, 2016 (received for review July 27, 2016)

Only a small fraction of vitamin B_{12}-requiring organisms are able to synthesize B_{12} de novo, making it a common commodity in microbial communities. Initially recognized as an enzyme cofactor of a few enzymes, recent studies have revealed additional B_{12}-binding enzymes and regulatory roles for B_{12}. Here we report the development and use of a B_{12}-based chemical probe to identify B_{12}-binding proteins in a nonphototrophic B_{12}-producing bacterium. Two unexpected discoveries resulted from this study. First, we identified a light-sensing B_{12}-binding transcriptional regulator and demonstrated that it controls folate and ubiquinone biosynthesis. Second, our probe captured proteins involved in folate, methionine, and ubiquinone metabolism, suggesting that it may play a role as an allosteric effector of these processes. These metabolic processes produce precursors for synthesis of DNA, RNA, and protein. Thereby, B_{12} likely modulates growth, and by limiting its availability to auxotrophs, B_{12}-producing organisms may facilitate coordination of community metabolism.

chemical biology | cobalamin | metabolism | microbial regulation

Vitamin B_{12} encompasses a group of closely related corrinoid compounds best known for their role as cofactors of enzymes that mediate methyl transfer reactions, isomerase rearrangements, and dehalogenation (1). Although a common B_{12}-binding motif can be used to mine sequences for the presence of novel B_{12}-dependent enzymes (2, 3), new enzymes that lack the canonical motif continue to be discovered (4). Vitamin B_{12} also regulates protein expression by binding to riboswitches (5), which are regulatory RNA. These riboswitches primarily attenuate synthesis of proteins associated with B_{12} biosynthesis and salvage, but recent studies in the human microbiome suggest that nearly half of the 4,000 riboswitch-regulated proteins discovered are not associated with these processes, suggestive of considerable discovery opportunities (2). Recent studies have also revealed that vitamin B_{12} is a cofactor of transcriptional regulators and antirepressors (2, 3, 6). The upper portion of vitamin B_{12} is photolabile; thus, when bound to these proteins, it provides light-dependent regulation of transcription, controlling processes, such as biosynthesis of carotenoids, tetrapyrroles, and photosystems (6, 7).

The de novo biosynthesis of B_{12} occurs only in bacteria and archaea, yet is used by all domains of life (8). B_{12} is energetically costly, requiring nearly 30 different enzymes for its synthesis (1, 9), which likely explains why only a small fraction of prokaryotes have the genetic capacity to produce it. In natural microbial communities, from eukaryote-associated to those occurring within terrestrial, aquatic, or other environments, the limited sources of B_{12} makes it a precious commodity (10). As such the availability of, and access to, B_{12} has been suggested to impart a fundamental contribution to their spatial and functional organization (3).

To examine the role of metabolic interactions in community structure and function, we developed two nearly identical model photoautotrophic microbial consortia derived from a naturally occurring aquatic mat (11). Each consortium consists of one distinctive photosynthetic cyanobacterium and up to 18 heterotrophic bacteria. Through genome annotation we have identified extensive vitamin B_{12} auxotrophy among the members, with only the cyanobacterium and three heterotrophs from each community capable of B_{12} biosynthesis (12). All three heterotrophs have been isolated and can also salvage B_{12}, and are therefore receptive to exogenously supplied B_{12} making probing of live cells with B_{12} mimics feasible. However, only one, *Halomonas* sp. HL-48 (hereafter, *Halomonas*), can be propagated in defined media in which levels of exogenously supplied B_{12} can be controlled.

Here we describe the development of an affinity-based vitamin B_{12} probe (B_{12}-ABP), and its in situ application to *Halomonas*. Our probe selectively captured 41 proteins from *Halomonas*, including enzymes known to use it as a cofactor, a transcriptional regulator, three enzymes in the one carbon pool by folate, and two enzymes in ubiquinone biosynthesis. We demonstrate that the captured regulator binds—in a light-dependent manner—a conserved DNA motif upstream to several genes, including four that are associated with either folate or ubiquinone biosynthesis. The unexpected discovery of B_{12} involvement in these processes suggests a pivotal role in the control of cell growth in response to

Significance

Using a chemical probe mimic of vitamin B_{12}, we reveal a light- and B_{12}-dependent DNA regulator, and make the unexpected discovery of B_{12} having regulatory involvement in microbial folate, ubiquinone, and methionine processes. These findings suggest a pivotal role for B_{12} in the control of cell growth, which may lead to coordination of cell behavior in complex multicellular systems. As key research questions emerge from host-associated and environmental microbiomes, we anticipate that B_{12} regulatory control of metabolism will be found to be generalizable, will be critical for coordination of individual microbe and community metabolism, and that organismal interdependencies for B_{12} may be pertinent to microbiome organization, stability, and overall function.

Author contributions: M.F.R., D.A.R., and A.T.W. designed research; Y.M., L.N.A., P.N., I.A.R., A.C., X.L., C.X., and T.R.W.C. performed research; P.N. contributed new reagents/analytic tools; M.F.R., D.A.R., Y.M., L.N.A., P.N., C.X., Y.-M.K., T.O.M., and A.T.W. analyzed data; and M.F.R., D.A.R., Y.M., L.N.A., P.N., and A.T.W. wrote the paper.

The authors declare no conflict of interest.

This article is a PNAS Direct Submission.

Freely available online through the PNAS open access option.

Data deposition: The mass spectrometry proteomics data have been deposited to the ProteomeXchange Consortium via the PRIDE partner repository with dataset identifiers PXD005723.

[1]M.F.R., D.A.R., and Y.M. contributed equally to this work.

[2]Present Address: Division of Biological Sciences, University of California, San Diego, La Jolla, CA 92093.

[3]To whom correspondence should be addressed. Email: aaron.wright@pnnl.gov.

This article contains supporting information online at www.pnas.org/lookup/suppl/doi:10.1073/pnas.1612360114/-/DCSupplemental.

photostress, potentially leading to coordination of cell behavior in complex multicellular systems.

Results

Development of an Affinity-Based B_{12} Probe That Mimics Natural Vitamin B_{12}. With the goal of conducting live-cell probe-labeling studies, we sought to develop a vitamin B_{12} affinity-based probe that would be recognized, transported, and bind proteins akin to native vitamin B_{12}. Prior research with fluorescent analogs of B_{12} found that modification of any of the carboxamide nitrogens emanating off the tetrapyrrole core resulted in moderate to severe impacts on protein binding affinity (13–15). However, modification of the ribose-5′-hydroxy moiety of the ribose sugar resulted in biologically well-tolerated B_{12} analogs (16–21). To enable covalent bond-forming reactions between B_{12}-ABP and target proteins, we developed a "linker" moiety to attach at the 5′-hydroxy position of B_{12} (Fig. 1*A*) (22). The linker, **3**, contains a diazirine for irreversible photo–cross-linking of the probe to B_{12}-binding proteins, and an alkyne group to enable click chemistry that is used in postlive cell labeling to append fluorophores for fluorescence measurements or biotin for enrichment of probe targets, and subsequent LC-MS analysis. B_{12}-ABP synthesis required four steps to develop the linker and append it to the ribose-5′-hydroxy position (Fig. 1*A*).

To confirm that the probe binds proteins akin to native B_{12}, we demonstrated that transcobalamin, a B_{12}-binding protein, was probe-labeled in a concentration-dependent manner and that the probe was outcompeted by addition of excess native cyanocobalamin (CNB_{12}) (Fig. S1*A*). Live cell uptake and protein labeling by B_{12}-ABP in *Halomonas* was experimentally validated by fluorescence gel analysis (Fig. S1*B*). We also expressed and purified the B_{12}-dependent enzyme, MetH, from *Halomonas* sp. HL-48 and demonstrated labeling by B_{12}-ABP and ablation of the binding upon addition of excess CNB_{12} (Fig. S2).

Affinity-Based Protein Profiling of *Halomonas* sp. HL-48. Our analyses (12) of the *Halomonas* sp. HL-48 genome revealed that it encodes machinery for synthesis and salvage of B_{12} and three B_{12}-dependent enzymes; thus, we anticipated that our probe would capture proteins involved in these processes. B_{12}-ABP was added directly to live *Halomonas* sp. HL-48 cells after they had reached exponential growth in B_{12}-deplete defined media (Fig. 1*B*). After 60 min, cells were UV-irradiated to stimulate probe–protein covalent bond formation via the diazirine moiety on B_{12}-ABP. Probed proteins were enriched by biotin affinity purification and quantitatively analyzed by LC-MS–based proteomics. B_{12}-ABP labeling of proteins was also competed with addition of excess CNB_{12}, and the competition experiment was quantitatively analyzed by proteomics. Accounting for only those proteins in which excess native CNB_{12} results in statistically significant diminished B_{12}-ABP protein labeling, we identified a total of 41 proteins (summarized in Table 1; full details in Dataset S1). Five of these proteins are components of three enzymes known to use B_{12} as a cofactor,

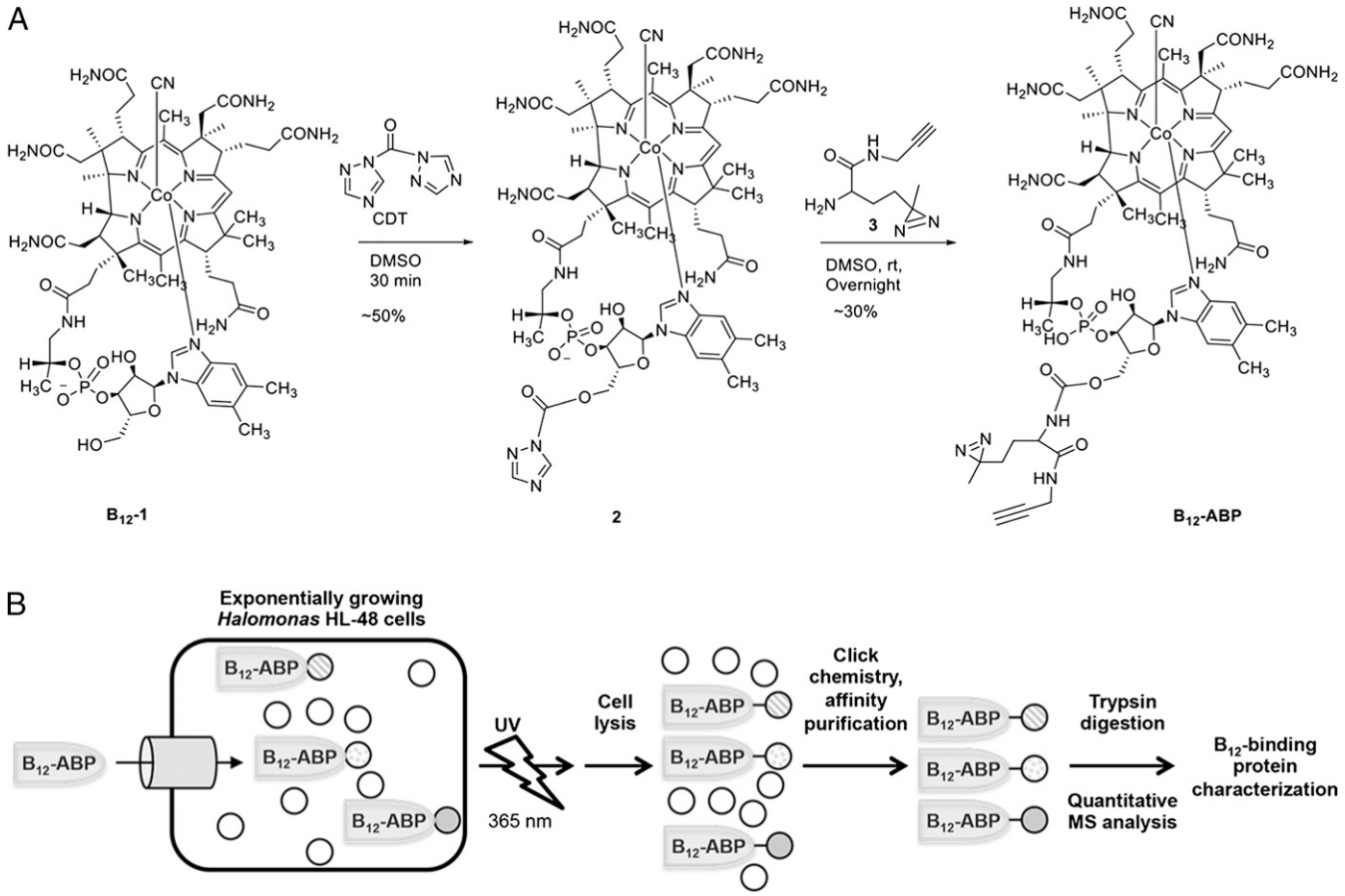

Fig. 1. B_{12}-ABP synthesis. (*A*) Cyanocobalamin (CNB_{12}) was converted to a photoreactive probe by carbamate bond formation to a linker moiety containing a diazirine and click chemistry-compatible alkyne. (*B*) B_{12}-ABP was added directly to live *Halomonas* cells, incubated for 60 min, then the samples were UV-irradiated to induce covalent bond formation between the probe and B_{12}-binding proteins. Cells were lysed, azido-biotin was added to probe-labeled proteins by click chemistry, and labeled proteins were enriched on a streptavidin agarose resin. Enriched proteins were digested on-resin, followed by quantitative LC-MS proteomic analysis of probe-labeled proteins by the accurate mass and time tag method.

Table 1. Categorization of 41 proteins detected by B_{12}-ABP

Functional category	No. of proteins	Protein designation
Nucleotide metabolism	2	NrdJa*, NrdJb*
Ethanolamine metabolism	2	EutB*, EutC*
Methionine metabolism	6	MetH*, MetE, LuxS, MsrB, MetK, MetZ
Porphyrin synthesis	3	HemE, CobW*, BtuR*
SAM/SAH-dependent enzymes	8	QueA, UbiE, UbiG, RlmI, RlmL, RlmN, RsmB, COG4106
Folate cycle	2	FolD, MetF
Regulation	2	PhrR, Mcp
Amino acid metabolism	2	DapC, AstB
Other systems	11	Hcp, Ssb, MmsA1, MmsA2, AptA, GatA, GapA, AtoB, RplN, TadA, CY41DRAFT_2254
Unknown function	3	CY41DRAFT_0508, CY41DRAFT_0804, CY41DRAFT_0947

*Proteins that are components of enzymatic complexes known to use B_{12} as a cofactor or substrate.

namely the methionine synthase (MetH), ribonucleotide reductase (NrdJa/NrdJb), and ethanolamine ammonia-lyase (EutB/EutC). The probe also detected cob(I)alamin adenosyltransferase (BtuR), an enzyme that reacts with B_{12} and its biosynthetic precursors as a substrate, catalyzing their adenylosylation during de novo biosynthesis or salvage. CobW, also bound by the probe, is known to be involved in B_{12} biosynthesis, but its exact function is still not clear. It has been proposed to be involved in cobalt insertion into a corrinoid precursor (23). It should be noted that we did not detect the vitamin B_{12} transporter, which we speculate is because of the low levels of the probe still retained on the transporter at the time UV was applied, or it may have been excluded from proteomic analysis because of it being a membrane component.

To confirm that probe-labeled proteins are not artifacts of the labeling process, proteomic controls were performed. First, samples treated with DMSO only (no probe), but for which all click chemistry steps were performed akin to the probed samples, were analyzed. Second, competition experiments with CNB_{12} were performed in which the B_{12}-ABP (2 μM) and CNB_{12} (100 μM) were added concomitantly to HL-48 proteins. The LC-MS proteomics data were analyzed, and the control samples were used to statistically validate probe labeling (Dataset S1). For additional validation, we expressed and purified FolD, MetE (Table 1), and MetH (positive control). These proteins were labeled with B_{12}-ABP, and labeling was competed by addition of excess CNB_{12} during the labeling experiment, which resulted in significantly inhibited or near complete ablation of labeling (Fig. S2). Additionally, the carbene generated by UV irradiation of the probe diazirine is rapidly protonated by water (24–26), so it is highly unlikely that the probe with the carbene moiety transiently diffused away from one protein through aqueous cytosol and incidentally labeled other proteins. As demonstrated by the labeling and competitive inhibition of purified MetH, FolD, and MetE, it is probable that the proteins identified in our proteomic measurements of B_{12}-ABP labeling do indeed rely on B_{12} binding, or they are in very tight multienzyme complexes. Finally, we also performed a global proteomic analysis of *Halomonas* HL-48 cells. When comparing the order of quantitative values from the global analysis to the B_{12}-ABP chemoproteomic analysis, meaning the highest to lowest values for the 41 B_{12}-binding proteins, they are correlative. This finding indicates that the probe labeling results in specific binding events, and does not follow the order of protein abundance; in fact, three proteins were not detected in the global proteome analysis that were identified by B_{12}-ABP chemoproteome analysis. In summary, our results confirm that the probe binds to and labels expected enzymes that require B_{12} as a cofactor or use it as a substrate, and identify 34 candidate B_{12}-binding proteins.

A Potential Allosteric Control Role for Vitamin B_{12}. Three probe-labeled proteins were identified that are involved at different points of the tetrapyrrole biosynthetic pathway that yields heme and B_{12} in *Halomonas*. The probe labeled uroporphyrinogen decarboxylase (HemE), which catalyzes the first reaction in heme biosynthesis from uroporphyrinogen III. This metabolite is also the precursor to vitamin B_{12} biosynthesis and, therefore, these anabolic processes compete for the same precursor. Allosteric control of HemE would provide *Halomonas* a means by which to control flux through these pathways based on B_{12} availability, and suggests a fundamentally new role for B_{12} in cellular metabolism. Prior reports on control of the tetrapyrrole biosynthetic pathway in other microbes have identified regulatory feedback controls by B_{12}-dependent riboswitches (27) and redox signaling cascades (28). Taking these data together, we find that vitamin B_{12} regulation of these steps could result in redirection of metabolism between biosynthesis of heme versus B_{12} biosynthesis.

B_{12} Interdependencies in Folate and Methionine Metabolism. Examination of additional enzymes bound by the B_{12}-ABP revealed a remarkable connection to processes linked by methionine synthase. Two variants of methionine synthase, MetH and MetE, are encoded by *Halomonas* and responsible for conversion of homocysteine to methionine (Fig. 2). Both enzymes were captured by the B_{12}-ABP, yet only MetH is known to depend on B_{12} for function. In many bacteria, MetE translation is repressed by an upstream cobalamin-binding riboswitch (29). In *Halomonas* the transcription of *metE* (CY41DRAFT_1840) is activated by MetR (CY41DRAFT_1841), but no upstream riboswitch for repression of MetE was detected (12). A new mechanism of control involving an allosteric interaction between MetE and B_{12} is suggested by our results. To confirm that MetE binds B_{12}, we expressed and purified the enzyme and labeled it with B_{12}-ABP, and also demonstrated that addition of excess CNB_{12} during the labeling experiment results in significantly inhibited probe labeling (Fig. S2). Additionally, given the number of replicate analyses that were performed, if probe labeling of the methionine cycle and 5-methyl tetrahydrofolate (5mTHF) recycling pathways was purely ancillary, the proteomic results would likely be highly variable, but they are not (Dataset S1).

The B_{12}-ABP also captured all three enzymes needed to synthesize 5mTHF, the methyl donor used in the MetH reaction, and five enzymes associated with methionine metabolism and repair (Fig. 2). These proteins are not known to be B_{12}-dependent; however, they are used in pathways that are linked by MetH and thereby may be probe-labeled because of close proximity effects. In correlation to the role B_{12} plays in methionine cycling, nine S-adynosyl methionine (SAM)-dependent enzymes were probe -labeled (Table 1). Most of these enzymes are methyltransferases involved in the modification of rRNA and tRNA, or synthesis of ubiquinone. In total, the B_{12}-ABP–labeling results point to significant and previously unknown roles in control of methionine and 5mTHF recycling, and the processes in which intermediates are used.

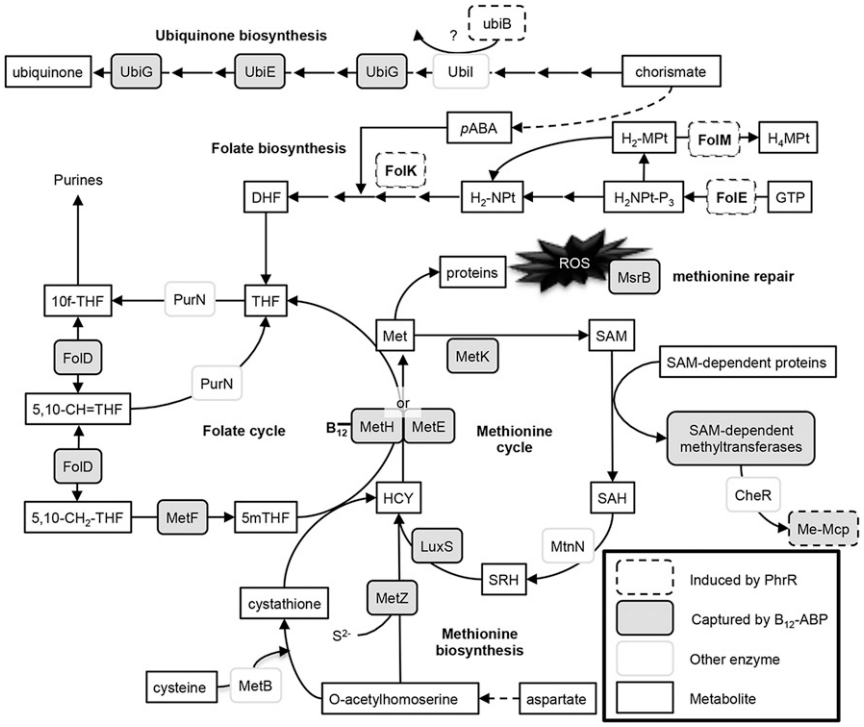

Fig. 2. B_{12}-ABP captures 17 proteins in methionine, folate, and ubiquinone metabolism. Metabolites are shown in open boxes: 5,10-CH = THF, 5,10-methenyltetrahydrofolate; 5,10-CH2-THF, 5,10-methylene-THF; 5mTHF, 5-methyl-THF; 10f-THF, 10-formyl THF; DHF, dihydrofolate; H_2-MPt, dihydromonapterin; H_4-MPt, tetrahydromonapterin; H_2-NPt-P3, dihydroneopterin triphosphate; H_2-NPt, dihydroneopterin; HCY, homocysteine; Met, methionine; pABA, p-aminobenzoate; SAH, S-adenosylhomocysteine; SRH, S-ribosylhomocysteine; THF, tetrahydrofolate;. Enzyme abbreviations: CheR, chemotaxis signal relay system methyltransferase; FolD, bifunctional methylenetetrahydrofolate dehydrogenase (NADP+)/methenyltetrahydrofolate cyclohydrolase; FolE, GTP cyclohydrolase; FolK, 2-amino-4-hydroxy-6-hydroxymethyldihydropteridine diphosphokinase; FolM, alternative dihydrofolate reductase 1; GlyA, glycine hydroxymethyltransferase; LuxS, S-ribosylhomocysteine lyase; MsrB, methionine-R-sulfoxide reductase; PurN, phosphoribosylglycinamide formyltransferase 1; MetE, B_{12}-independent methionine synthase; MetF, 5,10-methylenetetrahydrofolate reductase; MetH, B_{12}-dependent methionine synthase; MetK, S-adenosylmethionine synthetase; Me-MCP, methyl accepting chemotaxis protein; MtnN, adenosylhomocysteine nucleosidase; MetX, homoserine O-acetyltransferase; MetZ, O-succinylhomoserine sulfhydrylase; PanB, 3-methyl-2-oxobutanoate hydroxymethyltransferase; PurU, formyltetrahydrofolate deformylase; ThyA, thymidylate synthase; UbiB, ubiquinone biosynthesis monooxygenase; UbiG, bifunctional 2-polyprenyl-6-hydroxyphenyl methylase/3-demethylubiquinone-9 3-methyltransferase; UbiE, 2-methoxy-6-polyprenyl-1,4-benzoquinol methylase; UbiI, 2-octaprenylphenol hydroxylase. ROS, reactive oxygen species.

Identification of a B_{12}-Dependent DNA Transcription Factor PhrR. Probe labeling of *Halomonas* resulted in the identification of a B_{12}-dependent transcription factor from the MerR family, which was named PhrR (Table 1). Comparative genomics analysis of PhrR orthologs in Proteobacteria suggests that they belong to the previously uncharacterized group of light-controlled regulators of genes coding for DNA photolyases and other light dependent processes (see below). N-terminal DNA-binding domains in PhrR proteins are 41–49% similar to DNA-binding domains of the previously characterized B_{12}-dependent light-inducible regulators LitR from *Bacillus megaterium* and *Thermus thermophilus* and CarH from *Myxococcus xanthus* (30–32). However, PhrR proteins lack a canonical C-terminal B_{12}-binding domain, and would not be characterized as B_{12}-binding proteins by BLAST and domain searches using the trusted cutoff. B_{12} is known to act as a photosensitive regulator of transcription factors, where photolysis of B_{12} leads to altered DNA binding (7, 32). In *Halomonas* sp. and other Proteobacteria, orthologs of *phrR* are often colocalized on the chromosome with genes involved in photo-damage repair (*phr*) and cyclopropane fatty acid biosynthesis (*cfa*) (Fig. 3 and Dataset S2). Both of these activities are beneficial under light stress, further supporting the idea that PhrR is a B_{12}-dependent light-sensitive transcriptional regulator. Subsequently, we set out to more fully characterize the B_{12}-dependency, light regulation, and regulatory role of PhrR in *Halomonas*.

Reconstruction of PhrR Regulons in *Halomonas* and Other *Gammaproteobacteria*. Orthologs of *phrR* were identified in all 20 *Halomonas* species with sequenced genomes. In most of these genomes, *phrR* is clustered on the chromosome with the photolyase gene *phr*, suggesting it is a primary target gene for PhrR-dependent transcriptional regulation. We applied the comparative genomics approach to reconstruct the PhrR regulons. A conserved 21-bp palindrome was identified as a candidate PhrR-binding motif (Fig. 3*A*). The reconstructed PhrR regulons in the *Halomonas* genomes include several genes involved in light-dependent processes, such as DNA photolyases (*phr*, *phr2*), a blue light- and temperature-regulated antirepressor (*bluF*), the photoactive yellow protein (*pyp*), three folate biosynthesis genes (*folE*, *folK*, *folM*), two methyl-accepting chemotaxis proteins (*mcp1*, *mcp2*), one ubiquinone biosynthetic gene (*ubiB*), and several hypothetical enzymes and uncharacterized proteins (Fig. 3*B*; for detailed list of binding sites detected and domains and their putative functional roles, see Datasets S2 and S3). The comparative analysis of upstream gene regions in multiple *Halomonas* genomes (Fig. S3) suggests that PhrR likely functions as a repressor of its target genes, similarly to LitR and CarH (30–32).

Orthologs of *phrR* were also identified in several species that belong to other lineages of *Gammaproteobacteria*, where they are also colocated with *phr* (Fig. 3*C*). By applying a similar bioinformatics approach, we identified DNA binding site motifs for these PhrR orthologs (Fig. S4). In most of the genomes, the

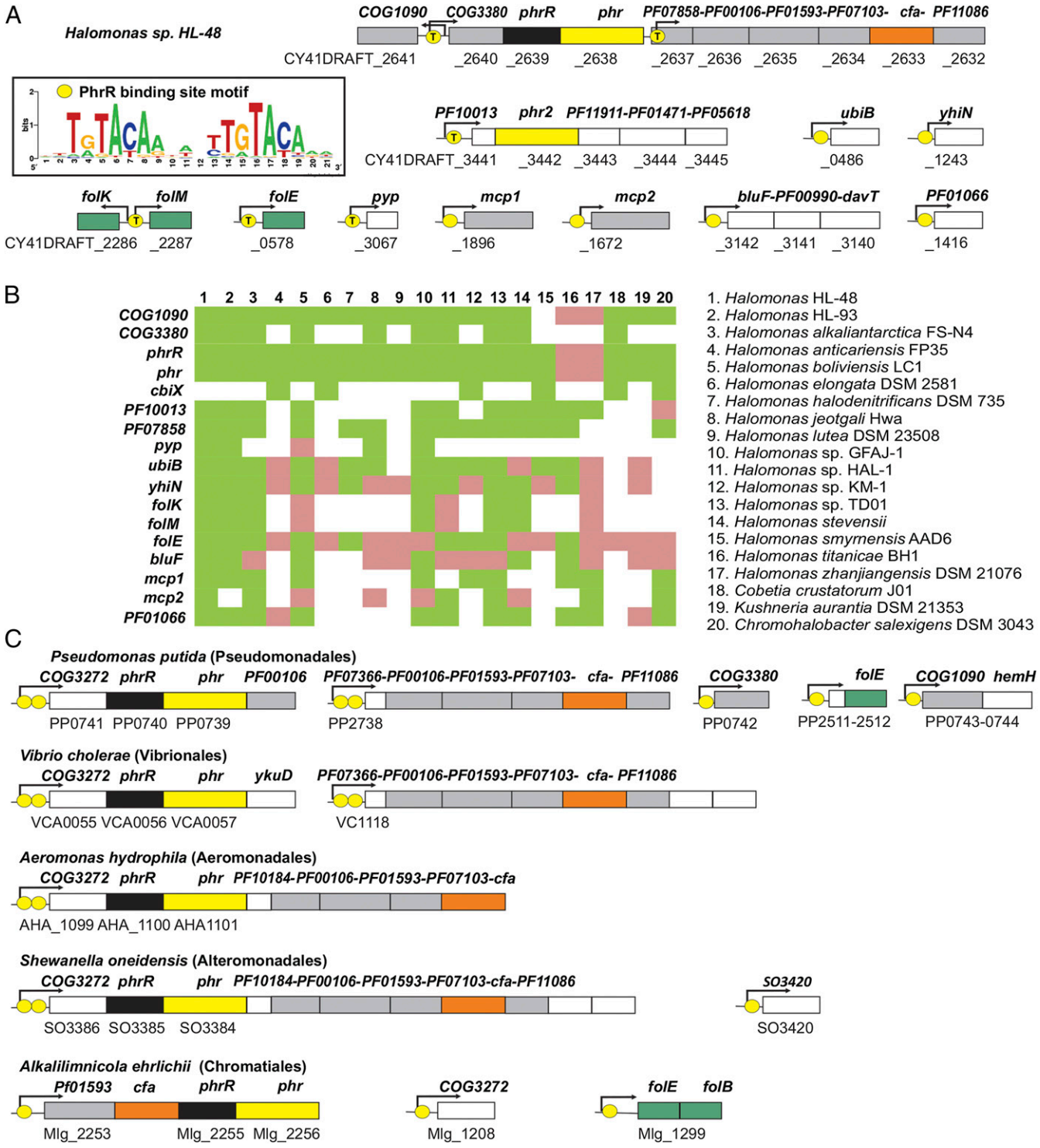

Fig. 3. Comparative genomics reconstruction of PhrR regulons in *Gammaproteobactreria*. (*A*) Predicted genes and candidate operons under regulation by PhrR in *Halomonas* HL-48. Genes, candidate PhrR-binding sites, and putative promoters are shown as rectangles, yellow circles, and small arrows, respectively. Sequence logo for PhrR-binding motif in the Halomonadaceae is shown in a box. Names and locus tags for PhrR-regulated genes are shown on top and bottom lines, respectively. The *phrR* (regulator) and *phr* (DNA photolyase) genes are in black and yellow, respectively. Genes in green and orange are involved in folate biosynthesis (*fol*) and cyclopropane fatty acid biosynthesis (*cfa*), respectively. Conserved members of the PhrR regulons in *Gammaproteobacteria* encoding functionally uncharacterized proteins (designated by Pfam/COG family numbers) are shown by gray rectangles. Experimentally tested PhrR sites are marked with a "T" in yellow circles. (*B*) Conserved core of PhrR regulons in 20 genomes of the *Halomonadaceae*. The table shows gene orthologs that are predicted to be regulated (light green squares) or not regulated (pink squares) by PhrR in each analyzed genome. The absence of a gene ortholog is shown by a blank space. (*C*) Genomic organization of PhrR-controlled loci in other *Gammaproteobacteria*.

reconstructed PhrR regulons control from one to four candidate operons (Datasets S2 and S3). This finding is in contrast with *Halomonas* spp., which possess up to 14 candidate PhrR-controlled operons per genome.

Structural Analysis of PhrR Proteins. The PhrR proteins from *Halomonas* species are distantly related to the B_{12}-dependent repressors CarH from *M. xanthus* and LitR from *T. thermophilus* and *B. megaterium*. LitR and CarH regulators are characterized by three Pfam domains: PF13411 (MerR HTH), PF02607 (B_{12}-binding-2), and PF02310 (B_{12}-binding). The PhrR proteins have highly conserved DNA binding domains from the MerR family, and their C-terminal domains are very weakly similar to those in LitR/CarH. The structure of the B_{12}-binding domains in the *T. thermophilus* LitR regulator was recently solved in complex with B_{12} (PDB ID code 3WHP) (7). We used the structure-based multiple alignment of the PhrR and LitR/CarH proteins to check the conservation of B_{12}-binding residues in their C-terminal domains (Fig. S5). Although the proteins seem to be structurally similar, the potential B_{12}-binding residues are not conserved in PhrR regulators. The histidine residue located in the beginning of the PF02310 domain, which was found to be functionally important in the previous studies of LitR and CarH proteins, is not conserved in any of the studied PhrR proteins. These observations suggest that the identified PhrR proteins in *Gammaproteobacteria* are characterized by highly diverged B_{12}-binding domains (often not detectable by Pfam search) that use a different pattern of residues for interaction with B_{12}. Future structure-functional studies will be required to identify these functionally important residues in the PhrR family.

Comparison of PhrR- and LitR-Binding DNA Motifs. The predicted lineage-specific PhrR-binding motifs demonstrated significant conservation across the analyzed taxonomic groups of *Gammaproteobacteria* (Fig. S4). The conserved consensus of palindromic PhrR motifs is TRTACAa-(flexible linker)-tTGTAYA. However, the length of internal linker between two conserved half-sites in PhrR motifs showed a remarkable flexibility. The PhrR half-sites are separated by 3 bp in the *Halomonadaceae*, *Chromatiales*/*Thiotrichales*, 9 bp in *Vibrionales* and *Marinomonas* spp., 10 bp in *Pseudomonadales*, and 11 bp in *Aeromonas* and *Shewanella* spp. Interestingly, the consensus half-site DNA motifs of PhrRs are similar to the experimentally determined DNA sites of the LitR regulators from *B. megaterium* and *T. thermophilus* (Fig. S4), however, the linkers between half-sites in the latter operators are 14 bp in length (30, 33). The similarity between half-site DNA motifs of PhrR operators correlates with high conservation of DNA-binding domains in PhrR and LitR (see above).

Functional Analysis of PhrR. To validate the computationally predicted DNA-binding motif of PhrR, we heterologously expressed and purified the PhrR protein from *Halomonas*. The recombinant PhrR protein exists partially as a dimer in solution (Fig. S6), supporting the hypothesis that the PhrR dimer binds to its cognate palindromic DNA motif. Additional spectrometry of the monomer fraction of PhrR incubated with fourfold molar excess of vitamin B_{12}, a prospective ligand of PhrR, demonstrated specific ligand binding to the protein (Fig. S7).

The interaction of the purified PhrR protein with its cognate DNA motif was assessed using a fluorescence polarization assay. The results show that PhrR specifically binds to the synthetic DNA fragment containing the consensus PhrR-binding site, TTGTACAAtttTTGTACAA (Fig. 4*A*). The apparent dissociation constant (K_d) value for the apo-PhrR protein interacting with the tested DNA fragment was 77 nM. The addition of potential ligands, CNB_{12} (2 μM) and adenosylcobalamin ($AdoB_{12}$, 4 μM), improved the PhrR–DNA complex formation, resulting in decreased K_d values, 57 ± 9 nM and 25 ± 8 nM, respectively. Titration of the effect of B_{12}-ABP and CNB_{12} on the interaction between PhrR (20 nM) and the DNA fragment revealed the apparent K_d values 4 ± 0.8 μM and 0.4 ± 0.2 μM for B_{12}-ABP and CNB_{12}, respectively (Fig. 4*B*), demonstrating that the probe binds B_{12}-dependent proteins akin to native vitamin B_{12}. We further tested the effect of illumination on the interaction of $AdoB_{12}$-PhrR with DNA. The dark-incubated $AdoB_{12}$-PhrR protein demonstrated specific binding to the consensus DNA motif, whereas illumination with white light for 5 min results in failure of PhrR to bind to the same DNA fragment (Fig. 4*C*). We also tested the interaction of $AdoB_{12}$-PhrR with six DNA fragments containing the predicted PhrR operators in *Halomonas* sp. HL-48 (Fig. 4 *D* and *E*). All tested DNA fragments demonstrated a concentration-dependent increase of fluorescence polarization, confirming specific interaction between the regulator and DNA fragments. As a negative control, we assessed the binding of PhrR with a DNA fragment containing a TrpR-binding site in *Halomonas* sp. HL-48. The apparent K_d values for the PhrR protein interacting with two high-scored PhrR binding sites from candidate promoter regions of the *CY41DRAFT_3441* and *CY41DRAFT_2637* genes were in the range of 30–40 nM, whereas the low-scored PhrR sites found upstream of the *pyp*, *phrR*, *folK*/*M*, and *folE* genes have showed the apparent K_d values 60 ± 10 nM, 77 ± 36 nM, 103 ± 30 nM, and 16 ± 6 nM, respectively. Finally, further confirming the interaction between B_{12} and PhrR, B_{12}-ABP labeling of purified PhrR is inhibited by addition of CNB_{12} (Fig. S2 and Dataset S1).

New Mode of Light-Dependent Global Gene Regulation Controlling Fatty Acid and Folate Biosynthesis. The comparative analysis of upstream promoter sequences in multiple *Halomonas* genomes (Fig. S4) suggests that PhrR functions as a repressor of its target genes. Thus, the PhrR regulon genes are predicted to be derepressed after exposure to light. To validate this bioinformatics prediction, we evaluated the gene-expression pattern of selected genes from the PhrR regulon by quantitative RT-PCR (qRT-PCR) analysis. The expression profiles of three folate biosynthetic genes (*folE*, *folK*, and *folM*) from two different growth conditions (either constant light or dark) were tested. All three genes tested showed up-regulation of expression when cells were grown in the light compared with those grown in the dark (Fig. 5*A*). These results indicate that the regulation of PhrR is similar to the recently described CarH (7), in which B_{12} serves as a light sensor to modulate its activities, thus resulting in light-dependent gene regulation.

To further validate the unexpected linkage between B_{12} and folate biosynthesis, we measured the intracellular concentrations of folate and its derivatives in wild-type *Halomonas* and a deletion mutant that lacked *phrR* grown in light or dark conditions. As anticipated, under light conditions wild-type *Halomonas* produced higher intracellular concentrations of tetrahydrofolate (THF) (Fig. 5*B* and Dataset S4). Light-responsive THF production was lost in the mutant and nearly all of the metabolite detected was THF, indicative of uncontrolled production of THF.

Our regulon analyses suggest that expression of a cyclopropane fatty acid (CFA) synthase gene is controlled by PhrR (Dataset S2). To confirm this prediction, cellular levels of CFAs were measured in wild-type and mutant *Halomonas*. Our results demonstrate that production of CFA in the wild-type was indeed higher during light growth (Fig. 5*C*) and that the mutant produced significantly more CFA than the wild-type, regardless of the growth condition.

Discussion

Previous to this study, vitamin B_{12} was recognized as a facilitator of enzyme function, a sensory component of transcriptional regulators that control functions required in light conditions, and an effector of riboswitches that repress protein synthesis. Using our B_{12}-ABP in a nonphotosynthetic organism, we validated that the probe captures proteins expected to interact with B_{12}. We also discovered a transcriptional regulator, PhrR, which uses B_{12} as a light sensor and identified genes and processes that are under its control, including several that are not obviously linked to light stress response. We also captured proteins with the B_{12}-ABP not expected

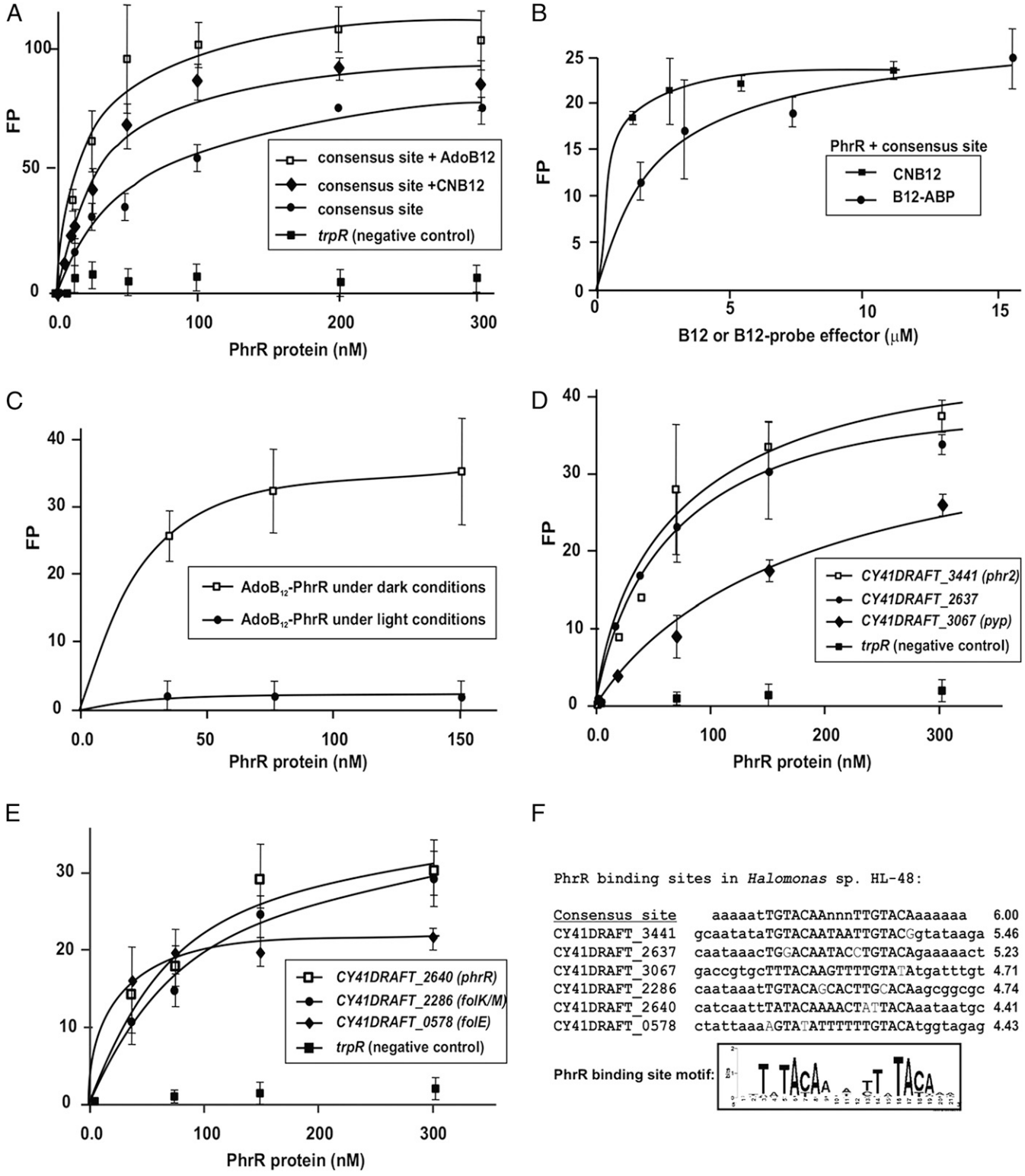

Fig. 4. Experimental validation of the PhrR regulon in *Halomonas* sp. HL-48 by fluorescence polarization (FP) binding assay. (*A*) Interactions between the recombinant PhrR protein and a DNA fragments containing consensus PhrR-binding site (6 nM) shows that DNA binding is specific and enhanced in the presence of CNB_{12} or adenosylcobalamin ($AdoB_{12}$). (*B*) Titration of the effect of B_{12}-ABP and CNB_{12} on the interaction between the recombinant PhrR protein (20 nM) and its predicted consensus DNA binding site (2.5 nM). (*C*) Light disrupts $AdoB_{12}$-dependent binding of PhrR to DNA. The PhrR protein (3 μM) was preincubated with $AdoB_{12}$ (66 μM) in the dark or irradiated with light for 5 min and then 0.7, 1.5, and 3 μM of the resulting PhrB:$AdoB_{12}$ complexes were checked for interaction with its consensus DNA motif (6 nM). (*D* and *E*) Effect of increasing concentrations of PhrR mixed with 33-bp DNA fragments (10 nM) containing candidate PhrR binding sites in the presence of $AdoB_{12}$ (4 μM). (*F*) Sequences of validated DNA fragments containing consensus PhrR-binding site and natural PhrR sites from *Halomonas* sp. HL-48 genome. Sequence logo represents the consensus PhrR-binding motif in the *Halomonadaceae*.

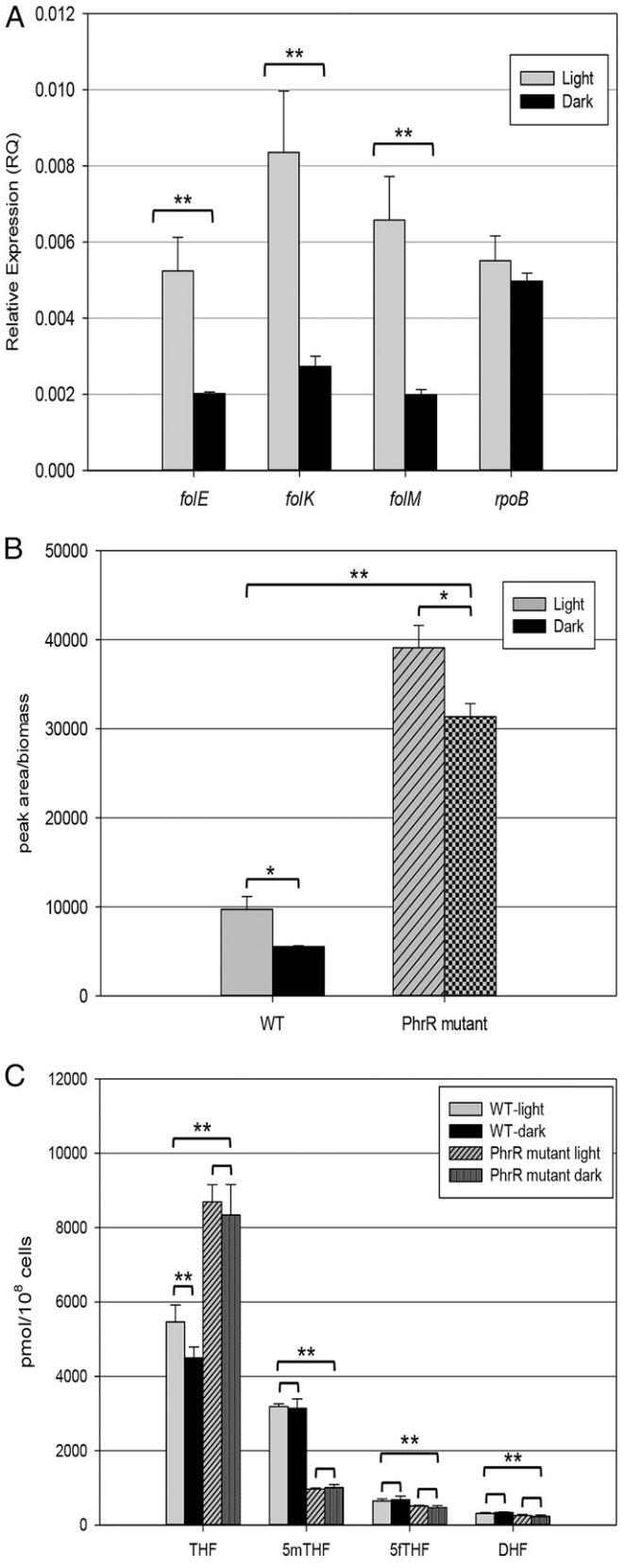

Fig. 5. Effect of light vs. dark growth conditions on *Halomonas* HL-48 gene expression and intracellular metabolite production. (*A*) Relative gene-expression levels of PhrR regulated folate genes; *rpoB* is a control not regulated by PhrR. $n = 3$. (*B*) Cyclopropane fatty acid levels determined by metabolomic analysis in WT *Halomonas* HL-48 and a *PhrR* mutant. $n = 3$. (*C*) Levels of folate derivatives; 5mTHF, 5-methyl tetrahydrofolate; 5fTHF, 5-formyl tetrahydrofolate; DHF, dihydrofolate. $n = 3$. Statistically significant differences in measured gene or metabolite levels in *A*–*C* were evaluated by *t* test ($n = 3$): one asterisk (*): $0.05 < P < 0.1$; two asterisks (**): $0.05 < P < 0.001$.

to bind B_{12}. A remarkable overlap was revealed in processes that were under control of PhrR or captured by the B_{12}-ABP; both were linked to ubiquinone biosynthesis, folate metabolism, and chemotaxis. The unprecedented connection between B_{12} and these processes suggest that B_{12} plays an even greater role in coordinating cellular metabolism than previously recognized.

We speculate that our results reflect a role for B_{12} as an allosteric regulator in *Halomonas*, controlling metabolic flux between B_{12} and heme biosynthesis, biosynthesis of ubiquinone, interconversions between THF and 5meTHF, and metabolism of methionine. THF metabolites produced by enzymes bound by B_{12}-ABP are used in the biosynthesis of purines, DNA, CoA, and serine. Control of these enzymes would consequently have significant impact on host metabolism. Our previous genomic analysis of *Halomonas* HL-48 revealed that it only requires B_{12} as a cofactor for ethanolamine biosynthetic genes and riboswitch control of the B_{12} salvage system, thus making it surprising that it can synthesize such an energetically costly metabolite (12). The additional use of B_{12} to control key metabolic processes could potentially justify the cost of making it and provide a means for this nonphototrophic organism to modulate its metabolism according to day/night cycles, like the cyanobacteria with which they coexist. Taken together, our findings weave an intricate web of B_{12} regulation on metabolism within *Halomonas*, and points to a fundamental requirement for B_{12} in cell metabolism, regulation, and protection.

As key research questions emerge from host-associated and environmental microbiomes, we believe our approach and results suggest that B_{12} may be critical for coordination of individual microbe and community metabolism, and organismal interdependencies for B_{12} may be pertinent to microbiome organization, stability, and overall function. We predict that these roles for B_{12} may be generalizable in myriad communities.

Materials and Methods

Chemical Synthesis of B_{12}-ABP. For full methodology and characterization, see *SI Materials and Methods*.

B_{12}-ABP Binding Assays with Transcobalamin. Transcobalamin (human transcobalamin 2, ACRO Biosystems), a known B_{12}-binding protein, was used to demonstrate probe selectivity and confirm that the probe and native B_{12} bind at the same site on transcobalamin. Transcobalamin (10 μM) in PBS was labeled with B_{12}-ABP (in DMSO) at 37 °C for 1 h, and UV-irradiated on ice at 365 nm immediately following probe labeling. For inhibition studies, transcobalamin (10 μM) in PBS was incubated with native CNB_{12} (10 or 20 μM) for 10 min, followed by addition of B_{12}-ABP (10 μM) for 30 min. The samples were then UV-irradiated on ice at 365 nm for 10 min. To characterize protein labeling and CNB_{12} competition by SDS/PAGE, we first incorporated tetramethylrhodamine onto the probe via click chemistry. Azido-tetramethylrhodamine fluorophore (2.65 μM) was added to probe-labeled protein solutions followed by the addition of Tris(2-carboxyethyl)phosphine; (22 μM), TBTA (Tris[(1-benzyl-1H-1,2,3-traizol-4-yl)methyl])amine) in a 4:1 solution t-butanol:DMSO (44.8 μM), copper sulfate (45 μM), and proteins were separated using 10% (wt/vol) Tris-Glycine SDS/PAGE gels. Fluorescence imaging was performed on a Protein Simple FluorchemQ system (Fig. S1*A*).

Live-Cell B_{12}-ABP Labeling of Proteins in *Halomonas* HL-48 Detected by Fluorescence. *Halomonas* strain HL-48 was grown at 30 °C in Hot Lake Heterotroph (HLH) broth, pH 8.0 (11). For B_{12}-ABP experiments, *Halomonas* was grown with shaking in 35 mL modified HLH defined medium lacking yeast extract and supplemented with 5 mM sucrose. At the mid-late log-growth phase, cells were collected by centrifugation (6,000 × *g*, 15 min) and used for live-cell probe labeling. To the pelleted cells was added 0.5 mL PBS with mild vortexing, followed by addition of B_{12}-ABP (10 μM, in 1 μL DMSO), which was incubated with the cells for 1 h at 30 °C. Following incubation, cells were UV-irradiated on ice at

365 nm for 10 min. Cells were washed with PBS (2 × 0.5 mL) and lysed by bead beating using a Next Advance Bullet Blender. Azido-tetramethylrhodamine-azide was added by click chemistry, as described above, and protein labeling was determined by fluorescence gel imaging (Fig. S1*B*).

Chemoproteomic Identification of B_{12}-ABP Binding Proteins, Competitive Inhibition Studies, and Global Proteomic Analysis of *Halomonas* HL-48. For quantitative chemoproteomic identification of B_{12}-ABP binding targets, probe labeling of *Halomonas* HL-48 cells ($n = 3$) was conducted as described for fluorescence gel imaging. In addition, three replicate experiments of competition labeling with CNB_{12} (50× probe concentration) were performed, as were three no-probe control experiments (addition of DMSO only), both to further confirm the identification of B_{12}-binding proteins (see *SI Materials and Methods* for additional details). Probe-labeled whole cells were immediately washed with PBS, fractionated, lysed, and azido-biotin was appended via click chemistry for subsequent enrichment of probe-labeled proteins on streptavidin agarose resin. For chemoproteomic and global proteomic analyses, proteins were digested by trypsin digestion for LC-MS analysis using our recently described methods (22, 34–36).

LC-MS Proteomic Measurement and Quantitative Characterization of *Halomonas* Proteins Captured by the B_{12}-ABP. Tryptic peptides from enriched proteins were separated on in-house manufactured reverse-phase resin columns by LC and analyzed on a Thermo Fisher Velos Orbitrap MS. Data were acquired for 100 min, beginning 65 min after sample injection into the LC. Spectra were collected from 400 to 2,000 *m/z* at a resolution of 100k, followed by data-dependent ion-trap generation of MS/MS spectra of the six most-abundant ions using collision energy of 35%. A dynamic exclusion time of 30 s was used to discriminate against previously analyzed ions. For full details of the data analysis, see *SI Materials and Methods*.

Gene Cloning and Purification of Recombinant PhrR, FolD, MetE, and MetH Proteins. The *phrR* gene (locus tag CY41DRAFT_2639) from *Halomonas* sp. HL-48 was amplified by PCR from genomic DNA using two primers containing the BamHI and HindIII restriction sites, 5′-gatcatggatccATGAGCAACAAGGCGACCCACCCACCCG, and 5′-gagtcgaagcttTCAAAGAACGCCCGATTCACGAAGCAACG. The PCR product was cloned into the pSMT3 expression vector and the recombinant PhrR protein was expressed with an N-terminal His_6-Smt3-tag in *Escherichia coli* BL21/DE3 under the T7 promoter.

The *folD* gene (locus tag CY41DRAFT_0662), partial *metH* gene containing B_{12} binding domain (2634bp) (locus tag CY41DRAFT_0722), and *metE* gene (Locus tag CY41DRAFT_1840) from *Halomonas* sp. HL-48 were amplified by PCR from genomic DNA using primer sets containing the BamHI and HindIII restriction sites for *folD* (5′-ggattaggatccATGACCGCCCAACTCATCGATGG, and 5′-ggatataagcttTTAATGGTTTTCGCGATCGTGCTGTTCGG), *metH* (5′-ggattaggatccTCGCTGTTCGTCAACGTCGGTGAACGC, and 5′-ggtataaagcttTTAGCTCGGGTCGTAAGACAGCACCGG), and BamHI and XhoI restriction sites for *metE* (5′-ggattaggatccATGACAGTTTCTCATATTCTCGGC, and 5′-ggtatactcgagTCAGGCGTAACGCGCGCGCAGTTGC). The PCR product of each gene was cloned into the pSMT3 expression vector and the recombinant FolD, MetH, and MetE proteins were expressed with an N-terminal His6-Smt3-tag in *E. coli* BL21/DE3 under the T7 promoter.

Recombinant proteins were purified to homogeneity using Ni^{2+}-chelation chromatography. See *SI Materials and Methods* for full details of cloning and purification.

Fluorescence Gel Analysis of B_{12}-ABP Labeling of Purified FolD, MetE, MetH, and PhrR Proteins. To further evaluate selectivity of the purified proteins PhrR, MetE, MetH, and FolD (each at 2 μM), proteins were labeled with B_{12}-ABP (2 μM) and competed with excess native CNB_{12} (10×, 25×, and 50× the B_{12}-ABP concentration) for 30 min at 30 °C. Following labeling, UV irradiation, click chemistry, and gel electrophoresis were performed as described for the transcobalamin-labeling experiment (Fig. S2). See *SI Materials and Methods* for additional experimental details.

DNA Binding Assays. The interaction of the purified recombinant PhrR protein with its cognate DNA binding sites in *Halomonas* sp. HL-48 was assessed using a fluorescence polarization assay. The 29-bp DNA fragment containing the predicted consensus DNA binding motif of PhrR and 33-bp DNA fragments of promoter regions of three PhrR target genes from *Halomonas* sp. HL-48 (Fig. 4) were synthesized (Integrated DNA Technologies). The double-stranded DNA (dsDNA) fragments were obtained by annealing synthesized complementary oligonucleotides at a 1:10 ratio of 5′-labeled with 6-carboxyfluorescein to unlabeled complementary oligonucleotides. Another 29-bp DNA fragment containing candidate site of TrpR repressor upstream of the *trpR* gene was used as a negative control. The labeled dsDNA fragments were incubated at 24 °C with the increasing concentrations of the purified PhrR protein (5–300 nM) in a 100-μL reaction mixture in 96-well black plates (VWR) for 20 min. The binding buffer contained 50 mM Tris buffer (pH 7.5), 0.1 M NaCl. Herring sperm DNA (1 μg) was added to the reaction mixture as a nonspecific competitor DNA to suppress nonspecific binding. The fluorescence-labeled DNA was detected with the FLA-5100 fluorescent image analyzer. The effect of adenosylcobalamin ($AdoB_{12}$) and cyanocobalamin (CNB_{12}) was tested by their addition to the incubation mixture. The effect of light was tested by incubation of 3 μM PhrR with 66 μM $AdoB_{12}$ in the dark or under white light conditions for 5 min followed by fluorescence polarization assay testing of the PhrR–DNA specific interaction. The PhrR-$AdoB_{12}$ mixture was illuminated by a white lamp in transilluminator (115 V, 0.37 Amp) in a 96-well transparent plate.

Genomic Reconstruction of PhrR Regulons. Orthologs of *phrR* (e.g., HELO_1271 in *Halomonas elongata*) were identified in all 17 *Halomonas* species with sequenced genomes. We applied the integrative comparative genomics approach to reconstruct the PhrR regulons in the genomes of *Halomonas* species (as implemented in the RegPredict Web server, regpredict.lbl.gov) (37). The approach combines identification of candidate regulator binding sites with cross-genomic comparison of regulons and with functional context analysis of candidate target genes (38). The upstream regions of all *phrR*-containing operons from 17 *Halomonas* species, as well as from three other representatives of the *Halomonadaceae* family, were analyzed using a DNA motif recognition program (the "Discover Profile" procedure implemented in RegPredict) to identify the conserved PhrR-binding DNA motif. The identified PhrR motif is a 21-bp palindrome. After construction of a positional-weight matrix for PhrR motif, we searched for additional PhrR-binding sites in the analyzed *Halomonas* genomes and performed a consistency check or cross-species comparison of the predicted PhrR regulons. The most conserved regulatory sites confirmed by phylogenetic footprinting approach (Fig. S4) were added to rebuild the positional weight matrix for PhrR sites. Scores of candidate sites were calculated as the sum of positional nucleotide weights. The score threshold was defined as the lowest score observed in the training set. Further genomic scans using the improved PhrR motif matrix resulted in final reconstruction of PhrR regulons in the *Halomonadaceae* spp.

Orthologs of PhrR proteins from *Halomonas* spp. were identified by BLAST searches against the nonredundant set of sequenced bacterial genomes and were further checked for their genomic context using the IMG database. PhrR orthologs were identified in several lineages of *Gammaproteobacteria*. In most cases, the *phrR* orthologs are located in the vicinity of the *phr* or *phrB* genes encoding DNA photolyases. Phylogenetic analysis of the PhrR-like proteins detected major groups of genomes encoding closely related PhrRs and provided a basis for PhrR binding site identification. For each group, we collected training sets of upstream DNA regions from the *phrR*-containing loci, identified conserved PhrR binding motifs, constructed a positional weight matrix, and searched for additional PhrR-binding sites in the genomes analyzed. Cross-species comparisons of the predicted sets of potentially regulated genes allowed us to tentatively define regulon composition for each analyzed lineage. The details of the reconstructed PhrR regulon are captured and displayed in RegPrecise, a specialized database of bacterial regulons (regprecise.lbl.gov) (39), as a part of the PhrR collection.

***phrR* Mutant Construction.** A markerless in-frame *phrR* deletion mutant of *Halomonas* HL-48 was constructed by crossover-PCR, as described previously (40, 41). The 500-bp DNA fragments encoding sequence flanking phrR were generated by PCR using primer pairs (upstream 5′-CAAACCCGGGCGCGAGCATCAGCCCGAAAGCC-3′ and 5′-GCGACGGTGTCCATTAGTGGCGGGCGCCAGTGCCTCTTAGTTG-3′; downstream 5′-GCCACTAATGGACACCGTCGCCGCGGCGGTGCCTCTCTCTGAACCG-3′ and 5′-GTGTCCCGGGAGCAAAGGCCACGGCGTCGTGG-3′), joined by overlapping extension PCR, and then cloned into plasmid pDS3.0 SmaI site. *E. coli* WM3064 was used for mating with HL-48 and primers that flanked the region targeted for deletion were used to identify desired mutants (5′-ATGACAGCAGCACAGACGTCGTCGC-3′ and 5′-CTAGGTGGACAGCGCCTTGAAGGC-3′).

CFA Analysis. Frozen *Halomonas* cell pellets were dried under vacuum. Next, 500 μL of 1.25 M HCl in methanol was added and the mixture incubated at 100 °C for 2 h to release free-fatty acids and convert them into fatty-acid methyl esters (FAMEs). Next, 500 μL of hexane was added to extract FAMEs, followed by addition of 500 μL water to the methanol layer to facilitate separation and extraction. After centrifuging for 5 min, the hexane layer collected and analyzed by GC-MS. For FAME data processing, peaks were matched and identified with two commercial databases, the NIST14 GC-MS

library and Wiley GC-MS FAME Database. A mixture of FAME chemical standards (Sigma-Aldrich, C8-C28) was analyzed before sample analysis, and their retention time information was used to correct the retention time of FAME peaks in samples.

Measurement of Intracellular Folate and Derivatives. The sample preparation procedure for folate extraction and analysis was performed with slight modifications as previously described (42). For full details see *SI Materials and Methods* and Dataset S4.

ACKNOWLEDGMENTS. This research was supported by the US Department of Energy (DOE), Office of Biological and Environmental Research (OBER), as part of BER's Genomic Science Program. This contribution originates from the Genomic Science Program Foundational Scientific Focus Area at the Pacific Northwest National Laboratory (PNNL). A portion of the research was performed using EMSL, a DOE Office of Science User Facility sponsored by OBER. PNNL is a multiprogram laboratory operated by Battelle for US DOE Contract DE-AC05-76RL01830. D.A.R. was also supported in part by the Russian Foundation for Basic Research (Award 14-04-00870) and by the Russian Academy of Sciences via the program "Molecular and Cellular Biology."

1. Roth JR, Lawrence JG, Bobik TA (1996) Cobalamin (coenzyme B_{12}): Synthesis and biological significance. *Annu Rev Microbiol* 50:137–181.
2. Degnan PH, Barry NA, Mok KC, Taga ME, Goodman AL (2014) Human gut microbes use multiple transporters to distinguish vitamin B_{12} analogs and compete in the gut. *Cell Host Microbe* 15(1):47–57.
3. Degnan PH, Taga ME, Goodman AL (2014) Vitamin B_{12} as a modulator of gut microbial ecology. *Cell Metab* 20(5):769–778.
4. Miles ZD, Myers WK, Kincannon WM, Britt RD, Bandarian V (2015) Biochemical and spectroscopic studies of epoxyqueuosine reductase: A novel iron-sulfur cluster- and cobalamin-containing protein involved in the biosynthesis of queuosine. *Biochemistry* 54(31):4927–4935.
5. Vitreschak AG, Rodionov DA, Mironov AA, Gelfand MS (2003) Regulation of the vitamin B_{12} metabolism and transport in bacteria by a conserved RNA structural element. *RNA* 9(9):1084–1097.
6. Klug G (2014) Beyond catalysis: vitamin B_{12} as a cofactor in gene regulation. *Mol Microbiol* 91(4):635–640.
7. Jost M, et al. (2015) Structural basis for gene regulation by a B12-dependent photoreceptor. *Nature* 526(7574):536–541.
8. Nielsen MJ, Rasmussen MR, Andersen CB, Nexø E, Moestrup SK (2012) Vitamin B_{12} transport from food to the body's cells—A sophisticated, multistep pathway. *Nat Rev Gastroenterol Hepatol* 9(6):345–354.
9. Warren MJ, Raux E, Schubert HL, Escalante-Semerena JC (2002) The biosynthesis of adenosylcobalamin (vitamin B_{12}). *Nat Prod Rep* 19(4):390–412.
10. Seth EC, Taga ME (2014) Nutrient cross-feeding in the microbial world. *Front Microbiol* 5:350.
11. Cole JK, et al. (2014) Phototrophic biofilm assembly in microbial-mat-derived unicyanobacterial consortia: model systems for the study of autotroph-heterotroph interactions. *Front Microbiol* 5:109.
12. Romine MF, Rodionov DA, Maezato Y, Osterman AL, Nelson WC, Underlying mechanisms for syntrophic metabolism of essential enzyme cofactors in microbial communities. *ISME J*, in press.
13. Petrus AK, Fairchild TJ, Doyle RP (2009) Traveling the vitamin B12 pathway: Oral delivery of protein and peptide drugs. *Angew Chem Int Ed Engl* 48(6):1022–1028.
14. Pathare PM, et al. (1996) Synthesis of cobalamin-biotin conjugates that vary in the position of cobalamin coupling. Evaluation of cobalamin derivative binding to transcobalamin II. *Bioconjug Chem* 7(2):217–232.
15. Russell-Jones GJ, Westwood SW, Farnworth PG, Findlay JK, Burger HG (1995) Synthesis of LHRH antagonists suitable for oral administration via the vitamin B12 uptake system. *Bioconjug Chem* 6(1):34–42.
16. Bagnato JD, Eilers AL, Horton RA, Grissom CB (2004) Synthesis and characterization of a cobalamin-colchicine conjugate as a novel tumor-targeted cytotoxin. *J Org Chem* 69(26):8987–8996.
17. Cannon MJ, et al. (2002) Equilibrium and kinetic analyses of the interactions between vitamin B(12) binding proteins and cobalamins by surface plasmon resonance. *Anal Biochem* 305(1):1–9.
18. Horton RA, Bagnato JD, Grissom CB (2003) Structural determination of 5′-OH alpha-ribofuranoside modified cobalamins via ^{13}C and DEPT NMR. *J Org Chem* 68(18):7108–7111.
19. Lee M, Grissom CB (2009) Design, synthesis, and characterization of fluorescent cobalamin analogues with high quantum efficiencies. *Org Lett* 11(12):2499–2502.
20. Smeltzer CC, et al. (2001) Synthesis and characterization of fluorescent cobalamin (CobalaFluor) derivatives for imaging. *Org Lett* 3(6):799–801.
21. Chromiński M, Gryko D (2013) "Clickable" vitamin B_{12} derivative. *Chemistry* 19(16):5141–5148.
22. Anderson LN, et al. (2016) Live cell discovery of microbial vitamin transport and enzyme-cofactor interactions. *ACS Chem Biol* 11(2):345–354.
23. Haas CE, et al. (2009) A subset of the diverse COG0523 family of putative metal chaperones is linked to zinc homeostasis in all kingdoms of life. *BMC Genomics* 10:470.
24. Richter G, Mendez-Vega E, Sander W (2016) Singlet halophenylcarbenes as strong hydrogen-bond acceptors. *J Phys Chem A* 120(20):3524–3532.
25. Chee G-L, Yalowich JC, Bodner A, Wu X, Hasinoff BB (2010) A diazirine-based photoaffinity etoposide probe for labeling topoisomerase II. *Bioorg Med Chem* 18(2):830–838.
26. Ford F, Yuzawa T, Platz MS, Matzinger S, Fülscher M (1998) Rearrangement of dimethylcarbene to propene: Study by laser flash photolysis and ab initio molecular orbital theory. *J Am Chem Soc* 120(18):4430–4438.
27. Rodionov DA, Vitreschak AG, Mironov AA, Gelfand MS (2003) Comparative genomics of the vitamin B_{12} metabolism and regulation in prokaryotes. *J Biol Chem* 278(42):41148–41159.
28. Zappa S, Li K, Bauer CE (2010) The tetrapyrrole biosynthetic pathway and its regulation in *Rhodobacter capsulatus*. *Adv Exp Med Biol* 675:229–250.
29. Kazanov MD, Vitreschak AG, Gelfand MS (2007) Abundance and functional diversity of riboswitches in microbial communities. *BMC Genomics* 8:347.
30. Takano H, et al. (2015) Role and function of LitR, an adenosyl B_{12}-bound light-sensitive regulator of *Bacillus megaterium* QM B1551, in regulation of carotenoid production. *J Bacteriol* 197(14):2301–2315.
31. Kutta RJ, et al. (2015) The photochemical mechanism of a B12-dependent photoreceptor protein. *Nat Commun* 6:7907.
32. Ortiz-Guerrero JM, Polanco MC, Murillo FJ, Padmanabhan S, Elías-Arnanz M (2011) Light-dependent gene regulation by a coenzyme B12-based photoreceptor. *Proc Natl Acad Sci USA* 108(18):7565–7570.
33. Takano H, et al. (2011) Involvement of CarA/LitR and CRP/FNR family transcriptional regulators in light-induced carotenoid production in *Thermus thermophilus*. *J Bacteriol* 193(10):2451–2459.
34. Wiedner SD, et al. (2012) Multiplexed activity-based protein profiling of the human pathogen *Aspergillus fumigatus* reveals large functional changes upon exposure to human serum. *J Biol Chem* 287(40):33447–33459.
35. Ansong C, et al. (2013) Identification of widespread adenosine nucleotide binding in *Mycobacterium tuberculosis*. *Chem Biol* 20(1):123–133.
36. Sadler NC, et al. (2014) Live cell chemical profiling of temporal redox dynamics in a photoautotrophic cyanobacterium. *ACS Chem Biol* 9(1):291–300.
37. Novichkov PS, et al. (2010) RegPredict: An integrated system for regulon inference in prokaryotes by comparative genomics approach. *Nucleic Acids Res* 38(Web Server issue):W299–W307.
38. Rodionov DA (2007) Comparative genomic reconstruction of transcriptional regulatory networks in bacteria. *Chem Rev* 107(8):3467–3497.
39. Novichkov PS, et al. (2013) RegPrecise 3.0—A resource for genome-scale exploration of transcriptional regulation in bacteria. *BMC Genomics* 14:745.
40. Gao W, et al. (2006) Knock-out of SO1377 gene, which encodes the member of a conserved hypothetical bacterial protein family COG2268, results in alteration of iron metabolism, increased spontaneous mutation and hydrogen peroxide sensitivity in *Shewanella oneidensis* MR-1. *BMC Genomics* 7:76.
41. Lee J, Lee HJ, Shin MK, Ryu WS (2004) Versatile PCR-mediated insertion or deletion mutagenesis. *Biotechniques* 36(3):398–400.
42. Patring JD, Jastrebova JA, Hjortmo SB, Andlid TA, Jägerstad IM (2005) Development of a simplified method for the determination of folates in baker's yeast by HPLC with ultraviolet and fluorescence detection. *J Agric Food Chem* 53(7):2406–2411.
43. Kim S, Gupta N, Pevzner PA (2008) Spectral probabilities and generating functions of tandem mass spectra: A strike against decoy databases. *J Proteome Res* 7(8):3354–3363.
44. Polpitiya AD, et al. (2008) DAnTE: A statistical tool for quantitative analysis of -omics data. *Bioinformatics* 24(13):1556–1558.
45. Shen Y, et al. (2004) Ultrasensitive proteomics using high-efficiency on-line micro-SPE-nanoLC-nanoESI MS and MS/MS. *Anal Chem* 76(1):144–154.